Analysis of the Proximal Orifice Flowfield Under Pulsatile Flow Conditions and Confining Wall Geometry:

Implications in Valvular Regurgitation

ANDREAS S. ANAYIOTOS, PH.D.,* POHOEY FAN, M.D.,† GILBERT J. PERRY, M.D.,†† JERRY MYERS, PH.D.,* ABDELAZIZ M. ELMAHDI, M.S.,* and NAVIN C. NANDA, M.D.†
*School of Engineering and †Division of Cardiovascular Disease, The University of Alabama at Birmingham; ††Cardiology Section, Birmingham Veteran's Administration Medical Center, Birmingham, Alabama

Hemodynamic studies of regurgitant lesions in the heart focus on identifying a reliable noninvasive method of volumetric flow calculation. In these studies the influence of blood viscosity to the flowfield under pulsatile flow conditions and constraining wall geometry has not been examined in detail. Pulsatile flow studies in straight tubes have shown that viscous effects significantly influence the periodic flowfield, especially near the wall. The purpose of this study is to investigate the significance of transient effects in the flowfield proximal to a lesion under constraining wall geometry. The proximal flowfield was analyzed with computational fluid dynamics (CFD) computer simulations and color flow Doppler mapping (CFM). Three different stroke volumes and regurgitant waveforms were investigated for upstream wall orientations that varied from – 64° to + 64° (measured from the orifice plane). Results showed that for each upstream wall orientation, a single instantaneously normalized centerline velocity distribution characterized the flowfield throughout the cycle. The centerline distributions were in phase with the pressure gradient and almost identical to the corresponding steady-state distributions. Minor deviations were observed near the wall, where viscous effects were predominant. Transient flow effects such as blunt profiles and pressure velocity phase shifts, which were observed in straight circular tubes, were not observed in regurgitant orifice flowfields. This is true even under severe confinement conditions. (ECHOCARDIOGRAPHY, Volume 15, April 1998)

valvular regurgitation, hemodynamics, numerical simulations, color flow Doppler mapping

Valvular regurgitation (VR) is a common dysfunction in heart patients. Cardiologists still pursue an accurate and reliable noninvasive method that will allow them to determine the volumetric amount of blood flow through the regurgitant orifice. Such a method would provide a better prognosis of the disease. Color flow Doppler mapping (CFM) remains the primary clinical tool in the qualitative evaluation of VR.

Efforts to provide a quantitative method of blood flow prediction through such orifices have not been successful yet. Originally, the region of the downstream regurgitant jet became the focus of numerous hemodynamic studies.[1-4] Several recent studies investigated the proximal orifice flowfield or the laminar approach region that consists of the proximal isovelocity surface areas or contours (PISA) that represent the acceleration of blood to-

This work has been partially supported by a grant from the Whitaker Foundation.

Address for correspondence and reprints: Andreas S. Anayiotos, Ph.D., The University of Alabama at Birmingham, Materials and Mechanical Engineering, BEC 358A, Birmingham, Alabama 35294. Fax: 205-934-8485.

wards the discharge orifice.[5-10] In vivo, regurgitant flowfields are influenced by valve leaflet and ventricular or aortic wall geometry. Such geometric factors in the presence of pulsatile flow conditions may considerably influence the development of the flowfield and the character of the PISA shapes. By the conservation of mass, PISA shapes are reduced in size and are closer to the orifice when the adjacent wall angle is negative (Fig. 1). The shapes elongate as the wall angle becomes positive.[11]

Numerical modeling of steady flow with various upstream wall orientations shows that the PISA shape changes with wall orientation. Rodriguez et al.[11] used clinical imaging and numerical modeling to investigate the funnel-like constraint on forward flow through stenotic mitral valves. Pu et al.[12,13] in a clinical study and an in vitro numerical model studied the impact of flow constraint in flail mitral leaflet.

According to Shandas et al.,[14] the shape of the PISA under pulsatile conditions does not change for an unbounded orifice. This has not been verified under severe confinement conditions, however. The effect of wall pulsatility under severe confinement conditions was not studied in detail by all the previously referenced studies. The proximity of the wall to the flowfield may bring considerable viscous effects similar to effects observed in straight circular tubes.

According to Womersley,[15] pulsatile effects significantly alter the laminar parabolic steady flow profile characteristics in circular tubes. Womersley determined that in a circular tube, such as a blood vessel, the unsteadiness characteristics are described by the dimensionless parameter:

$$\alpha = \frac{D}{2}\sqrt{\frac{2\pi f}{\upsilon}}$$

where D represents the vessel diameter, f the pulse frequency, υ the kinematic viscosity, and α the unsteadiness parameter or Womersley number. This parameter provides a measure of the relationship between viscous and unsteadiness effects. Even though the significance of this parameter has been studied extensively in arterial models, it has not been investigated for orifice flow.

Shandas et al.[14] used laser Doppler velocimetry to investigate the variation in centerline distribution for unbounded orifices under pulsatile conditions. They discovered that general steady flow characteristics of the centerline distribution held throughout the pulsatile cycle at > 1 diameter from the orifice. The initial and final stages of the cycle showed minor deviations.

This study investigates the influence of viscous effects for different adjacent wall orientations. The proximal orifice flowfields in steady and pulsatile flow environments are compared when the wall geometry adjacent to the orifice is changed from unbounded to + 64° confinement, as shown in Figure 1. Such comparisons can identify the presence of transient viscous effects.

The primary flow feature investigated was the centerline velocity distribution. Changes in the centerline distribution easily illustrate changes in wall orientation and provide a convenient means of comparison of the proximal flowfield. Utsunomiya et al.[8] reported the superiority of the general hemielliptical model to a simple hemispherical model in calculating flow across the flow convergence region. The idea of the proximal centerline distribution was introduced by Giesler and Stauch.[6] Under severe confinement conditions, the shape of the PISA close to the wall was also investigated.

Several investigators have been using the simple PISA technique to calculate flow

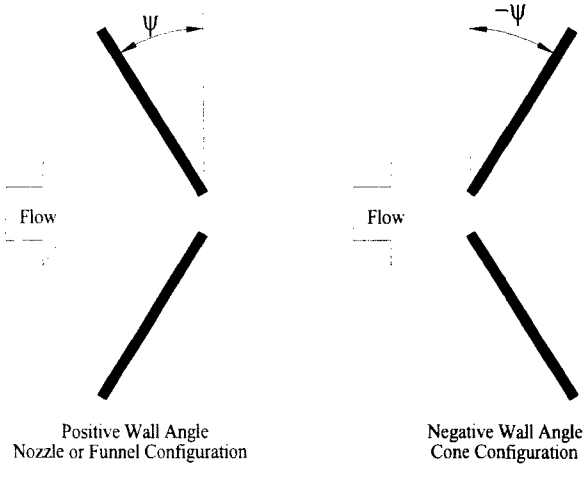

Figure 1. *Wall angle orientation measured relative to the orifice plane.*

through such restrictive orifices. Flow is calculated as follows: flow = (PISA) × velocity.[5-8] However, errors associated with the accuracy of the method have been reported in both in vitro and in vivo studies.[16-20] Such errors include variable PISA shape and velocity measurement errors. Under severe confinement conditions, viscous effects may influence the PISA shape additionally. The intention of this study is to (1) assess the proximal orifice flowfield when the adjacent wall changes geometry, and (2) assess the contribution of viscous effects to the shape of the isovelocity contours and the centerline velocity profile.

Methodology

Flowfields proximal to axisymmetric orifices with varying adjacent wall geometries were modeled using computational fluid dynamics (CFD) techniques. These simulations were performed for both steady and periodic flow conditions and compared to CFM interrogations of similar flowfields.

Numerical Simulations

CFD models were developed using the finite element method (FEM), which is a numerical procedure for determining approximate solutions of differential equations. FIDAP, a commercially available CFD software package provided by Fluid Dynamics International (Evanston, IL, USA), was used to develop FEM simulation of the steady and periodic proximal orifice flowfields. A 486-66 MHz PC accomplished the generation (geometry and mesh), preparation (boundary and initial conditions), and postprocessing of the CFD model. A CRAY C90 supercomputer was made available by the Alabama Research and Education Network in Huntsville, Alabama, for the performance of numerical solutions. In each of these simulations, the proximal flowfield was modeled as axisymmetric. Figure 2 illustrates the planar orifice model. The bottom line in the figure represents the line of symmetry at the model centerline. Hence, simulation of only a single halfplane of the solution domain is needed to define the flowfield. In the proximal region between the inlet and orifice, the FEM mesh is graded to obtain a very fine mesh in the region close to the orifice (Figs. 2 and 3). This results in a sparse mesh throughout the rest of the domain. Mesh grading allows the FEM simulation to track the large accelerations expected close to the orifice more accurately. This is done without significant increase in computational requirements. Figure 2 shows the nonplanar orifice models used.

An extension of the solution domain is positioned downstream of the orifice (Figures 2 and 3). The main function of this extension is to move the outlet plane, and thus the outlet boundary conditions away from the orifice plane.

For the steady flow studies seven different wall orientations were used for Ω = + 64°, + 47°, + 24°, 0°, – 24°, – 47°, – 64°. This is shown in Figure 3. The positive and negative angle orientation is shown in Figure 1. The orifice was chosen as 1 cm in diameter, and the flows used were 9.9 L/min, 7.42 L/min, and 5 L/min. For the pulsatile flow studies only the Ω = + 64° wall orientation was used.

The waveform used in the simulation is shown in Figure 4. The waveform modeled a regurgitant period with an initial increase in pressure gradient and velocity to some maximum value. This was followed by a gradual drop to a minimum value until the regurgitant cycle ended. The period was 0.84 seconds. Three different stroke volumes were used: (1) 139, (2) 104, and (3) 70 mL. The corresponding peak orifice velocities were 322, 226, and 169 cm/sec, respectively. For the steady-state models, the steady flow amount used were determined as follows: (1) 139 mL/0.84 sec = 165 mL/sec or 9.9 L/min, (2)104 mL/0.84 sec = 7.42 L/min, and (3) 70/0.84 sec = 5 L/min.

In the development of each of the CFD simulations, the various flow conditions and geometries were normalized using the orifice diameter (1cm) and the orifice velocity. This resulted in a normalized flowfield.

Experimental Study (Color Flow Doppler Analysis)

The flow system and test section are shown in Figure 5. The test section consisted of a + 64° wall orientation orifice model representing se-

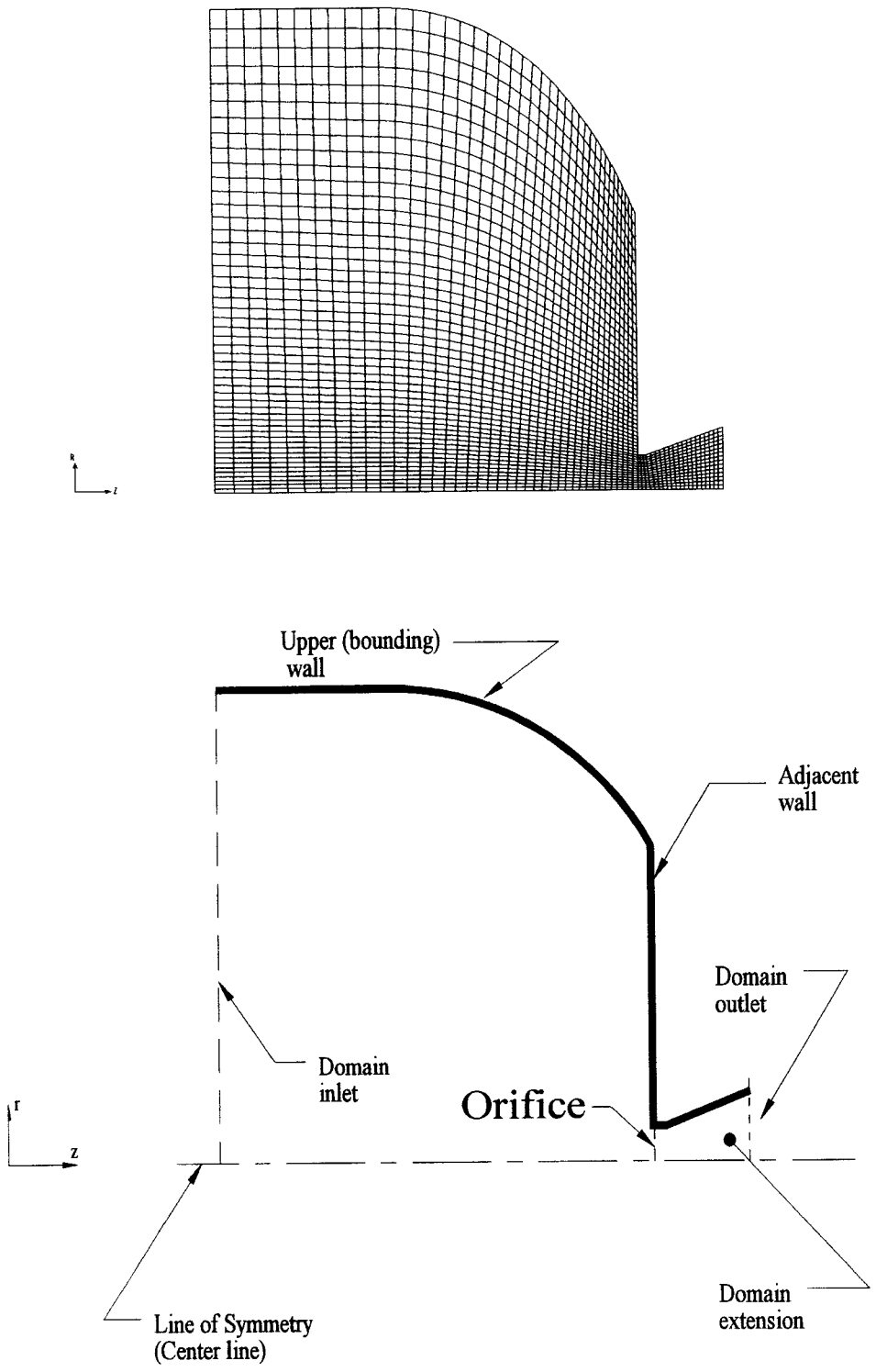

Figure 2. *Domain geometry and mesh distribution for the planar numerical orifice model. Only half the flowfield was modeled illustrating the axisymmetric nature of the geometry. The bottom line represents the centerline and line of symmetry. The orifice is to the right, followed by the extension. This was done to avoid application of the outlet boundary conditions right at the orifice.*

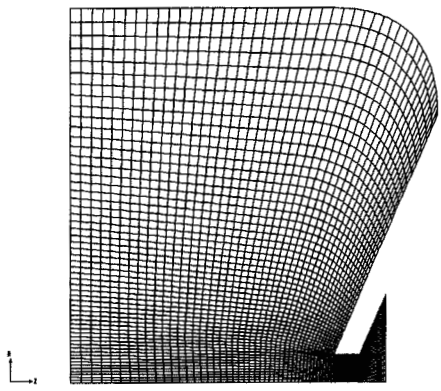

a) -24° wall angle (12081 nodal points)

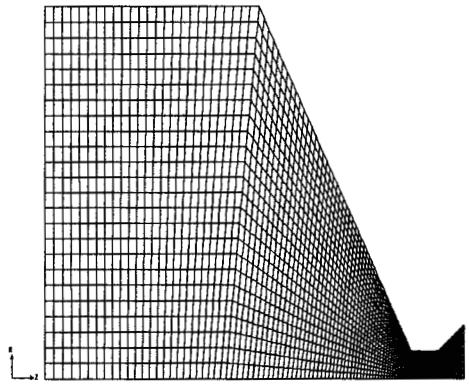

d) 24° wall angle (9751 nodal points)

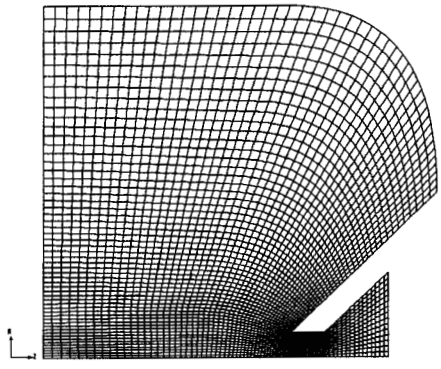

b) -47° wall angle (13047 nodal points)

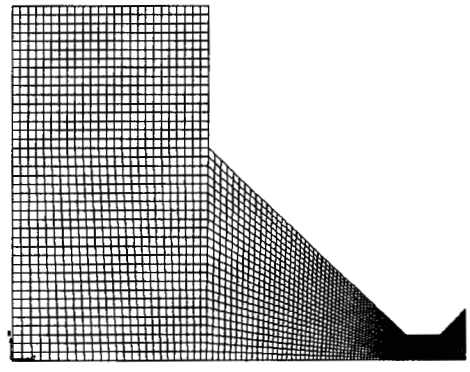

e) 47° wall angle (11383 nodal points)

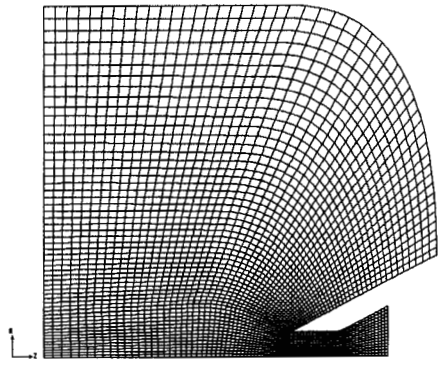

c) -64° wall angle (13047 nodal points)

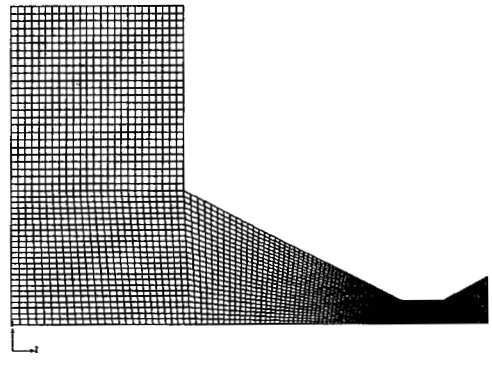

f) 64° wall angle (12301 nodal points)

Figure 3. *Domain geometry and mesh distribution for the nonplanar numerical orifice model.*

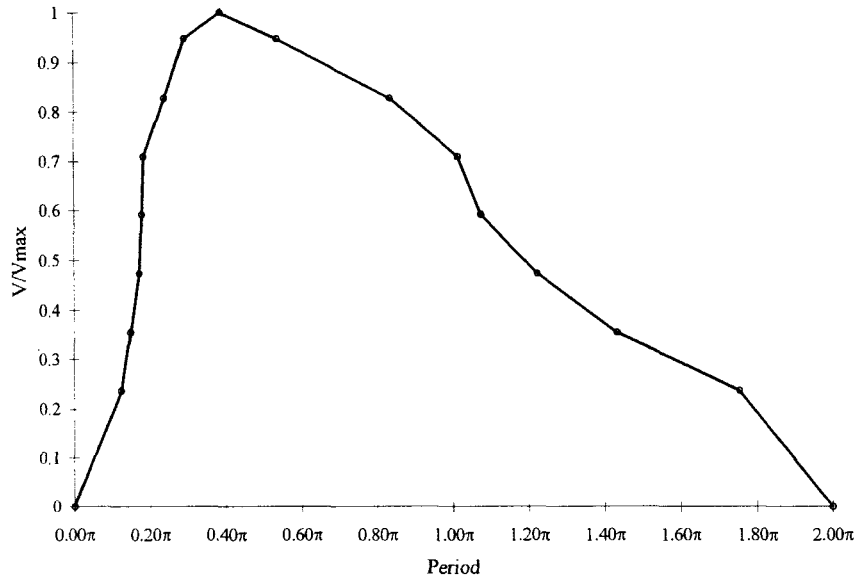

Figure 4. *The waveform used in the numerical simulations and experimental studies. It is normalized with the maximum velocity and the period (T = 0.84 sec) is subdivided in radians from 0 to 2π.*

vere confinement conditions in pulsatile flow. The flow waveform originated at the harvard pump and was modified to the desired shape by the compliance chambers to obtain the shape shown in Figure 4. The conditions used in the numerical simulation model were duplicated. The period was 0.84 sec, and three different stroke volumes were used: (1) 139, (2) 104, and (3) 70 mL. The corresponding peak orifice velocities were 322, 226, and 169 cm/sec, respectively. The contraction coefficient was 0.77 for this geometry and was determined experimentally.

The flow was monitored by an electromagnetic flowmeter probe and the pressure differ-

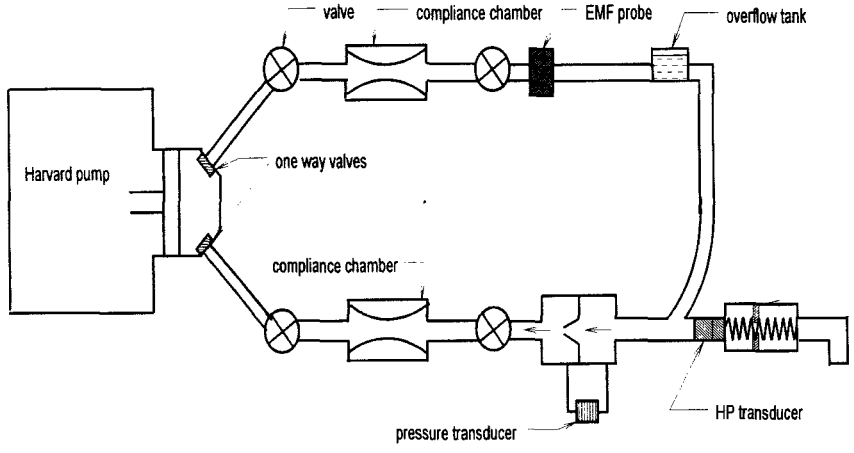

Figure 5. *The flow system used in the experimental study. The waveform is produced at the Harvard pump, and the compliance chambers are used to modify the waveform to a more physiological shape. The flow is monitored by an electromagnetic flowmeter and the pressure with a pressure transducer.*

ence across the orifice by a pressure transducer. The fluid used was an aqueous solution of glycerine (40% glycerine by weight). This provided a representative blood viscosity for the flow conditions used.

Velocity information was obtained using a Hewlett-Packard 2500 SONOS (Andover, MA, USA) DSR CFM Imaging System. M-mode CFM images were stored and retrieved using a digital program provided by Hewlett-Packard. The details of the program are explained in references 10 and 17. The Nyquist limit (NYL) was set between 30 and 100 cm sec^{-1}. CFM data from different NYL acquisitions of the same field were combined to cover the widest attainable range of velocities while maintaining the highest possible accuracy. The orifice location was at 9 cm from the transducer. The transducer was aligned along the centerline axis of the orifice (parallel to the axis of the regurgitant jet) at an imaging depth of 10 cm. Only centerline velocities (along the orifice axis) were analyzed using the M-mode feature of the instrument. The location of the color pixels were corrected for the difference between the velocity of ultrasound in the experimental fluid (1730 $msec^{-1}$) and human blood (1540 $msec^{-1}$). The correction factor was validated by measuring known distances by two-dimensional echo in the in vitro model. The color gain was adjusted about 30 dB and was kept constant throughout the study. This setting was enough to avoid background noise. Spatial filters were set to the off setting. Clutter filter was set on low (lowest wall filter setting) and packet size was set on medium. The definition setting of the instrument was set on high. Velocities were corrected for the effects of wall filters and spatial beam expansion as previously described in reference 17.

Results

The CFD simulations of the varying wall orientation and steady flow models were used to generate the plots of the PISAs as shown in Figure 6. Figure 7 shows the centerline velocity profiles. The velocity was normalized with average orifice velocity and the distance was normalized with orifice diameter. The purpose of this normalization is to be able to compare all the different geometric and flow cases on one graph. The centerline velocity profile represents the acceleration characteristics of each flow case. Figure 7 shows the significant change in velocity gradients with positive wall orientations when centerline distributions are compared with the zero angle case, which is the planar orifice model. Negative wall orientations however, showed little change in velocity gradient in comparison with the zero angle case. The agreement of the CFD numerical simulations with color Doppler data is manifested in Figure 8. Two centerline velocity distributions are compared, one for 0° wall orientation and the other for 64° wall orientation. The agreement between the numerical and CFM data is excellent.

Using the time-dependent flow waveform of Figure 4 and a wall orientation of $\Omega = +64°$, the pulsatile flow simulations indicated the contours shown in Figure 9. The contours correspond to normalized velocities of $v_i^* = 0.05$, 0.075, 0.1, 0.2, and 0.3. The contours are illustrated for 5 phases (ϕ) during the regurgitant cycle. The regurgitant cycle was subdivided in radians (0–2π radians). Three different stroke volumes were modeled (139, 104, and 70 mL), and the same contour shapes were obtained. Contour shapes appear identical in each phase of the cycle except for $\phi = 3\pi/2$, where minor changes were observed close to the wall. This was also confirmed by the centerline velocity profiles in Figure 10. Figures 9 and 10 indicate that the normalized contours and centerline profiles for all phases of the regurgitant cycle are essentially identical to the corresponding steady flow contours and centerline profiles.

The pulsatile flow findings of the numerical simulations were confirmed by color flow Doppler data. This is demonstrated in Figures 11A–11C. The graphs represent the centerline velocity distribution at the peak phase of the regurgitant cycle. Figure 11A shows the comparison for a pulse rate of 71 pulses/min, peak velocity of 169cm/sec, and stroke volume of 70 mL. The corresponding steady flowrate equivalent at this phase was 4.96 L/min. The NYL

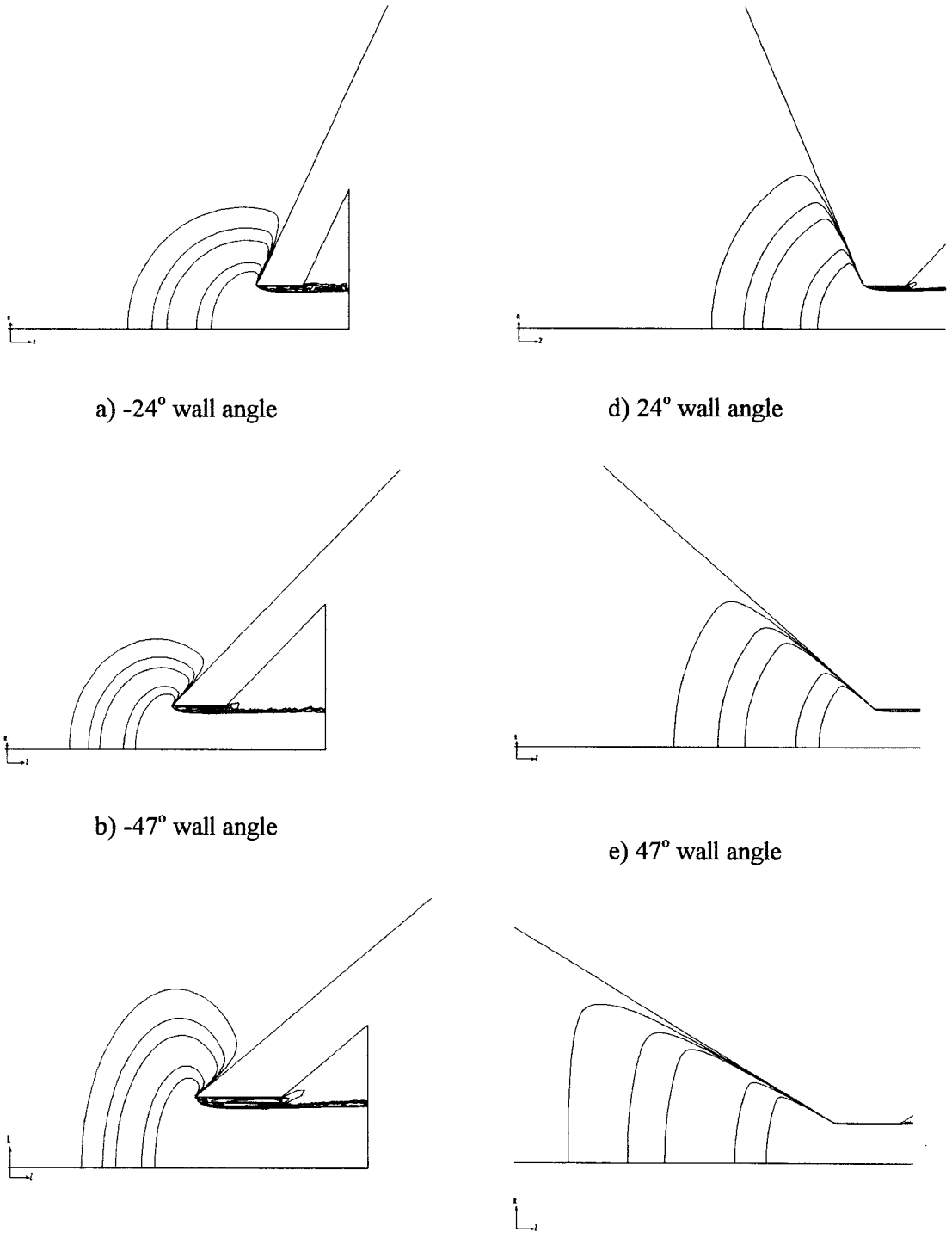

Figure 6. *Illustration of the isovelocity surfaces for a varying wall orientation model under steady conditions. The isovelocity contours shown are for a normalized velocity of V* = 0.05, 0.075, 0.1, 0.2, and 0.3.*

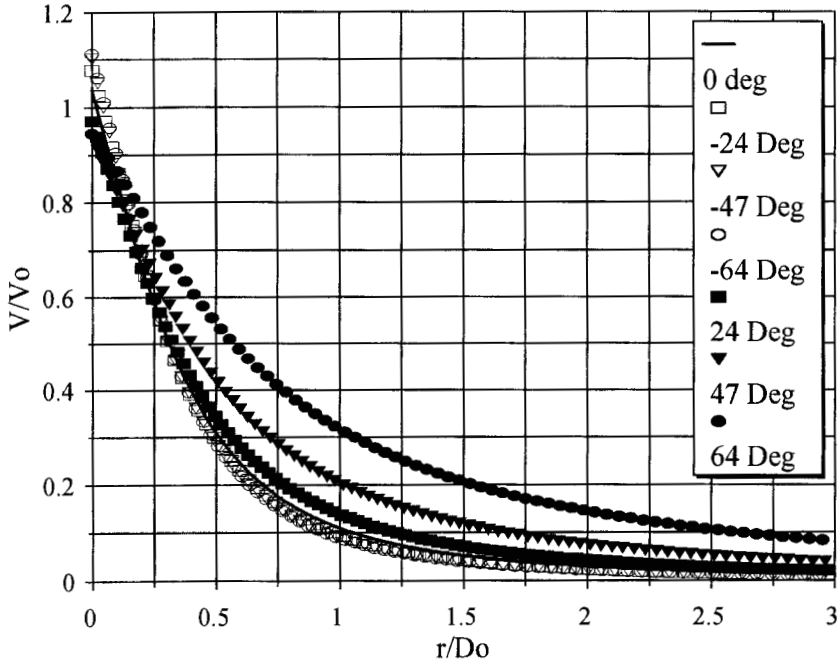

Figure 7. *Normalized centerline velocity distributions for a varying wall orientation. Distance from the orifice is normalized with orifice diameter (D_0); velocity is normalized with average orifice velocity (V_0).*

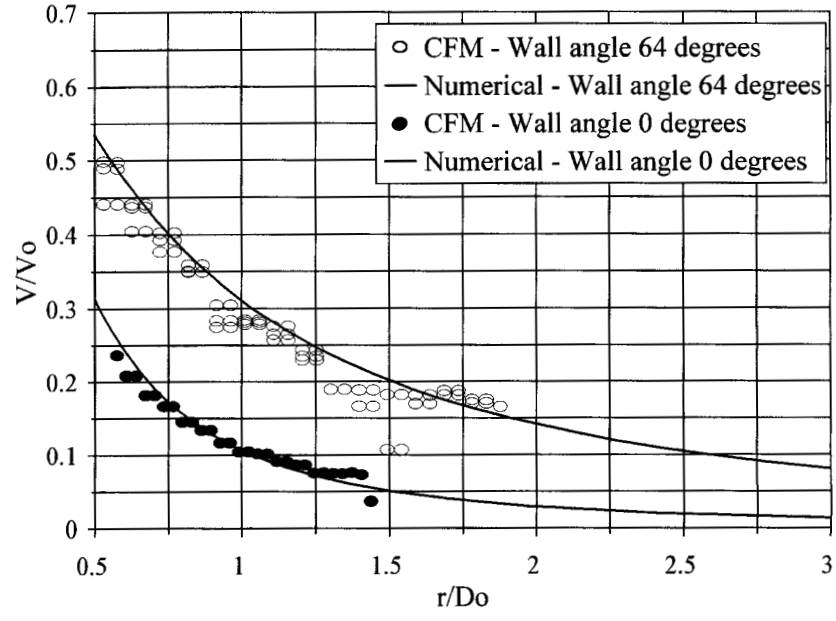

Figure 8. *Comparison of CFD simulations and CFM data for the normalized centerline velocity distribution. The upper curve refers to Ω =+ 64° wall orientation and the lower curve to Ω = 0° wall orientation.*

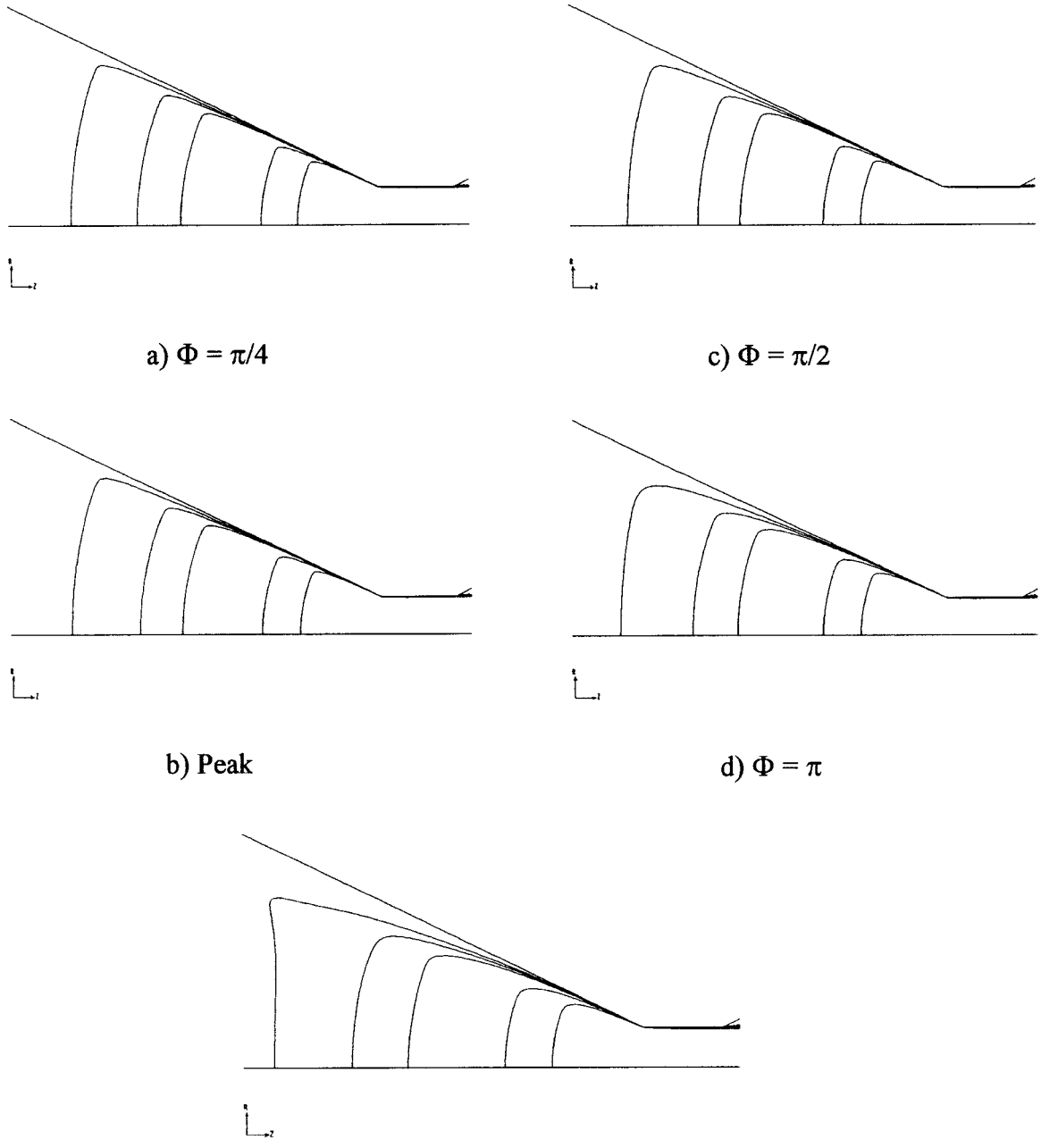

Figure 9. *Isovelocity contour behavior at five phases of the regurgitant cycle. The wall orientation is Ω =+ 64°, and the regurgitant cycle was T = 0.84 sec. The stroke volume was 139 mL and the peak velocity 339cm / sec.*

used was 65 cm/sec. The unsteadiness parameter was α = 6.5. Figure 11B shows the same comparison of velocity distribution when the stroke volume is 104 mL and the corresponding peak orifice velocity 226 cm/sec. NYL was 103 cm/sec. Similarly, Figure 11C shows the case of stroke volume = 139 mL and peak velocity = 322 cm/sec. NYL was 130 for this case.

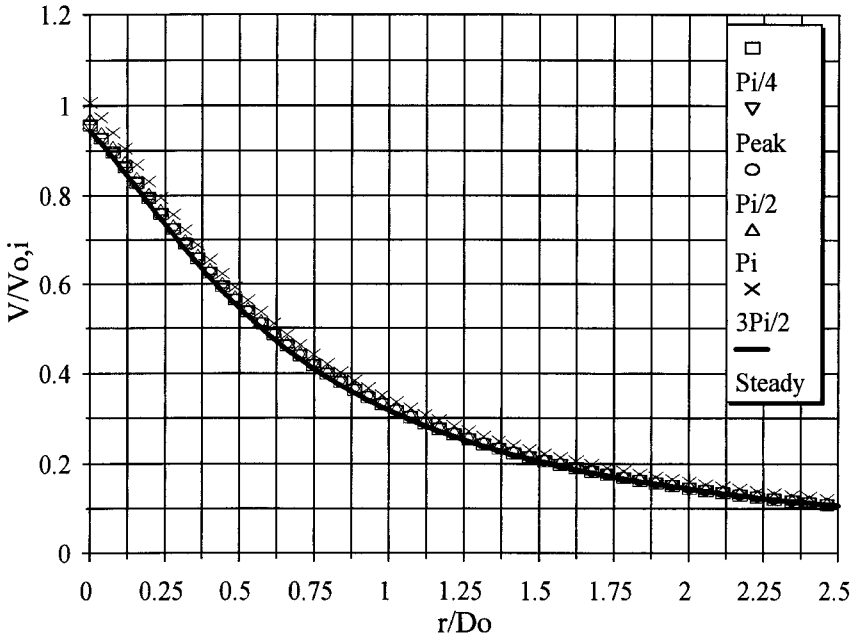

Figure 10. *Centerline velocity profiles at five phases of the regurgitant cycle and the corresponding steady flow profile. This curve clearly indicates identical results for each phase upon normalization.*

All figures illustrate the good agreement between the numerical and experimental data. The temporal velocity variation and comparison is shown in Figure 12. The time history of the velocity at a spatial location 0.47 diameters from the orifice is shown throughout the cycle. This was chosen to be a point near the orifice where the maximum allowable NYL could still provide nonaliased velocities. The color Doppler velocities appear to closely follow the numerically estimated velocities.

Discussion

The positive wall angle models appear to influence the spatial characteristics of the flowfield more than the negative wall angle models. In Figures 6 and 7 it is observed that the models with wall angle + 24°, + 47°, and + 64° provide higher velocities and smaller accelerations at the same locations along the centerline. This is a direct result of the conservation of mass. Since the wall confines the flow, the velocity increases to make up for the same amount of flow. The gradual change in velocity implies a smaller value of the velocity gradient or acceleration. For the negative wall angle models of wall angles – 24°, – 47°, and – 64°, the wall does not provide a confining effect, hence the centerline velocity distribution was essentially identical to the 0° wall distribution. From the fluid dynamics perspective, even though the negative wall angle models have the same distribution as the 0° wall angle, a higher pressure gradient is required to produce the same amount of flow through the orifice. Our positive angle data agree with corrections specified in Vandervoort et al.[20] Vandervoort et al. stated that α/π is the correction for flow through a wall constraining angle of I where $\alpha = 2\pi$ (1-cosI). However, our data show that no correction is required for the negative angle geometries since the centerline velocity profile of the zero angle model is the same as the profile for the negative angle models.

The pulsatile simulations and experimental studies focused on the wall constraining model of + 64°. It was expected that the temporal effects would impose a distortion on the flowfield due to the greater contribution of viscous effects in the presence of a confining wall.

Womersley[15] postulated that pulsatile flow in

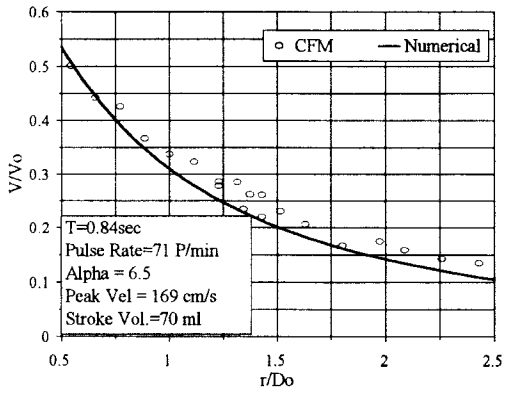

A

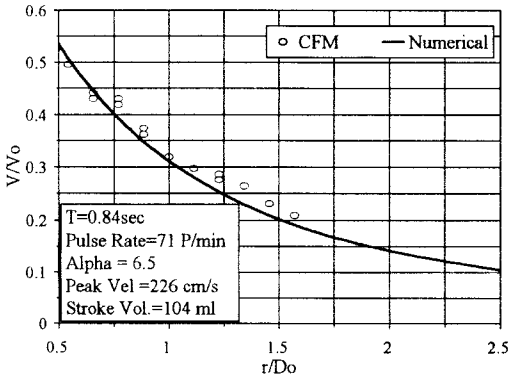

B

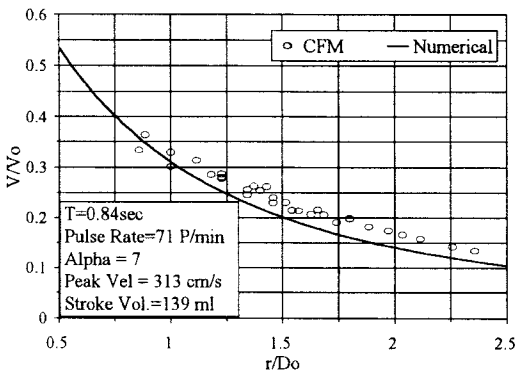

C

Figure 11. *(A) Comparison of centerline velocity at the peak phase of the regurgitant cycle. Diameter = 10 mm; NYL = 65 cm/s; equivalent steady flowrate = 5 L/min. (B) Comparison of centerline velocity at the peak phase of the regurgitant cycle. Diameter = 10 mm; NYL = 103 cm/s; equivalent steady flowrate = 7.42 L/min. (C) Comparison of centerline velocity at the peak phase of the regurgitant cycle. Diameter = 10 mm; NYL = 124 cm/sec; equivalent steady flowrate = 9.9 L/min. NYL = Nyquist limit.*

a circular pipe will have significantly different characteristics than steady flow. This study investigated the effect of pulsatile flow in a funnel orifice model where viscous effects are expected to predominate, as opposed to a planar orifice. A comparison of velocity/distance profiles under pulsatile conditions at different phases of the regurgitant flow waveform with corresponding steady velocity/distance profiles showed little difference. Figure 10 illustrates the comparison of the numerical pulsatile profile at different phases during the cycle to the corresponding steady profile. The isovelocity contours in Figure 9 appear to be identical upon normalization, except after the peak phase in the regurgitant cycle. For $\phi = 3\pi/2$ the contours appear to be distorted from their previous shape. In Figure 10, the change in the centerline distribution at this phase is detectable but small.

Figures 11A–11C show the peak regurgitant phase profile against the corresponding numerical steady profile obtained by CFM for three different flow cases. The experimental and theoretical agreement provides more credibility to the accuracy of the results of this study.

The close agreement between steady and pulsatile profiles shows that even in the presence of the wall, the combination of pulsatility and viscous effects do not alter the character of the flow. Doubling the frequency of oscillation in the numerical model resulted in no change of the flowfield. This agrees with results for an unrestricted orifice presented by Shandas.[14] Currently, the investigation is involved with numerical models with actual ventricular geometry and valvular flap motion.

Clinical Relevance and Limitations

The distortion of the flowfield in wall-restricted valvular regurgitation has been reported in previous studies.[11,14] The presence of ventricular wall or restricted flap motion may influence the proximal flowfield by distorting the shape of the isovelocity surfaces or centerline velocity profile. This distortion is predominantly attributed to the conservation of mass, which imposes a change on the flow character-

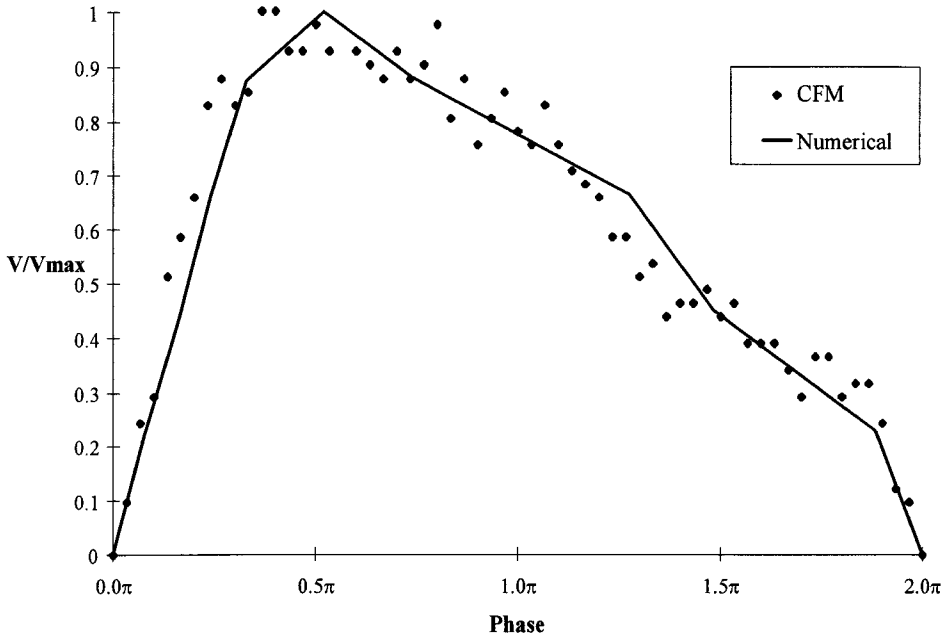

Figure 12. *Time history of the velocity waveform at r* = 0.47. The regurgitant cycle was T = 0.84 sec. The stroke volume was 139 mL and the peak velocity 339 cm/sec. α = 6.5. The M-mode velocity data closely follow the numerical simulation.*

istics in the presence of a geometric change, such as wall interference. This is equivalent to having channel flow rather than chamber flow. The imposed channel flow effect, however, does not introduce any temporal viscous effects as observed in flow through circular tubes (arterial flow).[18] Temporal viscous effects have been reported in the aortic arch and aortic bifurcation.[19,20] This phenomenon is not observed in this flow environment, as evidenced by preliminary experimental and numerical data. One of the reasons may be that regurgitant cycle flowfield is completely destroyed by the forward cycle flowfield before the next regurgitant cycle is repeated. This is not the case in arterial flow. The results of our study are limited by the fact that a funnel model was used with no moving walls or flaps. However this was considered to be the worst case scenario. Current experiments involve a realistic prosthetic tissue valve rather than a conical model, and the results of such studies will be reported in the near future. Only one representative regurgitant flow waveform was used; however, modeling other variations of regurgitant waveforms should not be considered as a limiting factor, since the transient effects are not expected to vary significantly from waveform to waveform.

Acknowledgments: The authors wish to thank the Whitaker Foundation for financially supporting this project.

References

1. Helmcke F, Nanda NC, Hsiung MC, et al: Color Doppler assessment of mitral regurgitation with orthogonal planes. *Circulation* 1987;75:175-183.
2. Cape EG, Yogonathan AP, Weyman AE, et al: Adjacent solid boundaries alter the size of regurgitant jets on Doppler color flow maps. *J Am Coll Cardiol* 1988;12:1354-1365.
3. Maciel BC, Moises VA, Shandas R, et al: Effects of pressure and volume of the receiving chamber on the spatial distribution of regurgitant jets as imaged by color Doppler flow mapping. An in vitro study. *Circulation* 1991;83:605-613.
4. Simpson IA, Valdes-Cruz LM, Sahn DJ, et al: Doppler color flow mapping of simulated in vitro regurgitant jets: Evaluation of the effects of orifice size and hemodynamic variables. *J Am Coll Cardiol* 1989;13:1195-1207.
5. Recusani F, Bargiggia GS, Yogonathan AP, et

al: New method for quantification of regurgitant flow rate using color Doppler flow imaging of the flow convergence region proximal to a discrete orifice. *Circulation* 1991;83:594-604.
6. Giesler MO, Stauch M: Color Doppler determination of regurgitant flow: From proximal isovelocity surface areas to proximal velocity profiles. *Echocardiography* 1992;9:51-62.
7. Rodriguez L, Anconina J, Flachskampf FA, et al: Impact of finite orifice size on proximal flow convergence: Implications for Doppler quantification of valvular regurgitation. *Circ Res* 1992; 70:923-930.
8. Utsunomiya T, Doshi R, Patel D, et al: Calculation of volume flow rate by the proximal isovelocity surface area method: Simplified approach using color Doppler zero baseline shift. *J Am Coll Cardiol* 1993;22:277-282.
9. Barclay SA, Eidenvall L, Karlsson M, et al: The shape of the proximal isovelocity surface area varies with regurgitant orifice size and distance from the orifice: Computer simulation and model experiments with color M-mode technique. *J Am Soc Echocardiogr* 1993;6:433-445.
10. Anayiotos A, Perry GJ, Myers JG, et al: A numerical and experimental investigation of the flow acceleration region proximal to an orifice. *Ultrasound Med Biol* 1995;21:4:501-516.
11. Rodriguez L, Thomas J, Monterroso V, et al: Validation of the proximal flow convergence method. Calculation of orifice area in patients with mitral stenosis. *Circulation* 1993;88:1157-1165.
12. Pu M, Vandervoot PM, Griffin BP, et al: Quantification of mitral regurgitation by the proximal convergence method using transesophageal echocardiography: Clinical validation of a geometric correction for proximal flow constraint. *Circulation* 1995;92:2169-2177.
13. Pu M, Vandervoot PM, Greenberg N, et al: Impact of wall constraint on velocity distribution in the proximal flow convergence zone: Implications for color Doppler quantification of mitral regurgitation. *J Am Coll Cardiol* 1996;27: 706-713.
14. Shandas R, Gharib M, Sahn DJ: Nature of flow acceleration into a finite-sized orifice: Steady and pulsatile flow studies on the flow convergence region using simultaneous ultrasound Doppler flow mapping and laser Doppler velocimetry. *J Am Coll Cardiol* 1995;25:1199-1212.
15. Womersley JR: The mathematical analysis of the arterial circulation in a state of oscillatory motion. Wright Air Development Center, Technical Report 1957;56-614,5-18.
16. Chen C, Koschyk D, Brockhoff C, et al: Noninvasive estimation of regurgitant flow rate and volume in patients with mitral regurgitation by color mapping of accelerating flow field. *J Am Coll Cardiol* 1993;21:374-383.
17. Perry GJ, Anayiotos AS, Green DW: Accuracy of color Doppler velocity in the flowfield proximal to a regurgitant orifice-implications for color Doppler quantification of valvular regurgitation. *Ultrasound Med Biol* 1996;22:605-621.
18. Vandervoort PM, Aghassi DS, Thomas JD: Impact of wall filtration on the accuracy of quantitative CFM velocity measurements: Numerical and in vitro study. *Adv Bioeng* 1992;22: 367-370.
19. Shiota T, Jones M, Teien DE: Evaluation of mitral regurgitation using a digitally determined Doppler flow convergence 'centerline' acceleration method. Studies in an animal model with quantified mitral regurgitation. *Circulation* 1994;89:2879-2887.
20. Vandervoort PM, Thoreau DH, Rivera JM: Automated flow rate calculations based on digital analysis of flow convergence proximal to regurgitant orifices. *J Am Coll Cardiol* 1993;22: 535-541.
21. Caro CG, Pedley TJ, Schroter RC, et al: The mechanics of the circulation. Oxford University Press, London, 1978.
22. Duncan D, Bargeron C, Borchart S: The effect of compliance on wall shear in casts of a human aortic bifurcation. *J Biomech Eng* 1990;5: 183-188.
23. Tarbell J, Klanchar M, Wang DM: In vitro study of the influence of radial wall motion on wall shear stress in an elastic tube model of the aorta. *Circ Res* 1990;66:1624-1635.